$^6P_{7/2}$-Excited-State Decay Mechanism and Energy-Transfer Processes in $KMgF_3:Eu^{2+}$ and $KMgF_3:Eu-X$ (X = Gd, Ce, Cr)

Haiquan Su, Zhihong Jia, and Chunshan Shi*

Key Laboratory of Rare Earth Chemistry and Physics, Changchun Institute of Applied Chemistry, Chinese Academy of Sciences, Changchun, China 130022

Ju Xin and S. A. Reid

Chemistry Department, Marquette University, Milwaukee, Wisconsin 53201-1881

Received March 1, 2001. Revised Manuscript Received July 9, 2001

A four-level decay model in $KMgF_3:Eu^{2+}$ is proposed. The decay profiles of the $^6P_{7/2}$ excited state of Eu^{2+} are biexponential, and the physical implication of each term in the fit equation responsible for the model is interpreted. The evidence obtained spectroscopically for supporting the model is presented. A new method to study energy transfer between Eu^{2+} and X^{3+} in $KMgF_3:Eu-X$ (X = Gd, Ce, Cr) is established on the basis of the proposed model.

I. Introduction

Optical transitions of divalent europium ($4f^7$) ions in $KMgF_3$ have been investigated extensively in many papers[1−12] due to the potential applications for phosphors or lasers.[13−17] Ellens et al.,[3] Francini and co-workers,[2] and Tsuboi et al.[1] suggest the existence of different possible sites for the impurity in $KMgF_3$. Although the majority of the divalent europium ions enter substitutionally in the crystal at a cubic site, other lattice sites of lower symmetry are available to europium, i.e., the tetragonal and trigonal symmetries. It is now well established that the presence of broad-band or line emission for Eu^{2+} depends on the coordination number, covalency, and crystal field strength at the Eu^{2+} site. Hence, the position of the $4f^65d$ state can be adjusted by changing the surrounding conditions of the Eu^{2+} ion. It was found that the $^6P_{7/2}$ state is at lower energy than the lowest $4f^65d$ state in $KMgF_3:Eu^{2+}$. However, the reported energy differences between the two states vary from author to author. Sardar et al.[5] estimated the value of 1250 cm^{-1} from a semilog plot of the $^6P_{7/2} \rightarrow {}^8S_{7/2}$ and $4f^65d \rightarrow {}^8S_{7/2}$ emission intensities versus T^{-1}. Altshuler et al.[12] found the value of 120 cm^{-1} from a fit to the temperature dependence of the $^6P_{7/2}$ decay time. Ellens and co-workers[3] obtained the value of 3350 cm^{-1} from spectral data and a fit to a three-level model involving $^8S_{7/2}$, $^6I_{7/2}$ and $4f^65d$ levels. They also suggested that the main reason for the erroneous result for ΔE_{fd} (the energy difference between the lowest $4f^65d$ level and the $^6P_{7/2}$ level, vide infra) for Eu^{2+} in the former two cases was that the results are fit to a three-level model including the $^6P_{7/2}$, $4f^65d$, and the $^8S_{7/2}$ levels. In reality more levels ($^6P_{5/2}$, $^6P_{3/2}$, and different $4f^65d$ levels) are involved. In the simple three-level model, the temperature dependence of the $^6P_{7/2} \rightarrow {}^8S_{7/2}$ transition probability (w_f in eq 2, vide infra), due to a change in the vibronic transition probability with temperature, is not taken into account. Hence, the values for ΔE_{fd} from fits to a three-level model are inaccurate. The spectroscopically determined values for ΔE_{fd}-($4f^65d-{}^6P_{7/2}$) are more accurate.

Recently we have begun to study the reason for this erroneous value of ΔE_{fd}. Several single crystals of $KMgF_3:Eu-X$ (X = Gd, Ce, Cr) and $KMgF_3:Eu^{2+}$ have been grown in our laboratory, and various optical measurements have been made. On the basis of the temperature dependence of lifetime, we propose a four-level decay model and a biexponential decay equation. Good agreement is found between the fit and the spectroscopic results. On the basis of this four-level model, many optical transition characteristics in $KMgF_3:Eu^{2+}$ can be interpreted, and the energy transfer between Eu^{2+} and other impurities in the codoped $KMgF_3$ system can be studied more efficiently.

* To whom correspondence should be addressed. E-mail: cshi@ciac.jl.cn. Fax: +86-0431-5685653.

(1) Tsuboi, T.; Scacco, A. *J. Phys.: Condens. Matter* **1998**, *10*, 7259.
(2) Francini, R.; Grassano, U. M.; Tomini, M.; Boiko, S.; Tarasov, G. G.; Scacco, A. *Phys. Rev. B* **1997**, *55*, 7579.
(3) Ellens, A.; Meijerink, A.; Blasse, G. *J. Lumin.* **1994**, *59*, 293.
(4) Garcia, J. M.; Sibley, W. A.; Hunt, C. A.; Spaeth, J. M. *J. Lumin.* **1988**, *42*, 35.
(5) Sardar, D. K.; Sibley, W. A.; Alcala, R. *J. Lumin.* **1982**, *27*, 401.
(6) Alcala, R.; Sardar, D. K.; Sibley, W. A. *J. Lumin.* **1982**, *27*, 273.
(7) Altshuler, N. S.; Livanova, L. D.; Stolov, A. L. *Opt. Spectrosc.* **1974**, *36*, 72.
(8) Dubiniski, M. A.; Livanova, L. D.; Stolov, A. L. *Sov. Phys. Solid State* **1980**, *22*, 711.
(9) Bodrug, S. N.; Valyashko, E. G.; Mednikova, V. N.; Sviridov, D. T.; Sviridov, R. K. *Opt. Spectrosc.* **1973**, *34*, 176.
(10) Altshuler, N. S.; Ivoilova, E. Kh.; Stolov, A. L. *Sov. Phys. Solid State* **1974**, *15*, 1602.
(11) Altshuler, N. S.; Korableva, S. L.; Stolov, A. L. *Sov. Phys. Solid State* **1976**, *18*, 679.
(12) Altshuler, N. S.; Korableva, S. L.; Livanova, L. D.; Stolov, A. L. *Sov. Phys. Solid State* **1974**, *15*, 2155.
(13) Lawson, J. K.; Payne, S. A. *Phys. Rev. B* **1993**, *47*, 14003.
(14) Kobayasi, T.; Mroczkowski, S.; Owen, J. F. *J. Lumin.* **1980**, *21*, 247.
(15) Blasse, G.; Wanmaker, W. L.; Ter Vrugt, J. W.; Bril, A. *Philips Res. Rep.* **1968**, *23*, 189.
(16) Blasse, G.; Bril, A. *Philips Technol. Rev.* **1970**, *31*, 304.
(17) Sommerdijk, J. L.; Bril, A. *J. Lumin.* **1970**, *10*, 145.

10.1021/cm0101881 CCC: $20.00
Published on Web 09/27/2001

II. Experimental Section

The crystals were grown by the vertical Bridgman method in graphite crucibles in an argon atmosphere. Europium, cerium, chromium, and gadolinium ions were added as EuF_3, CeF_3, Cr_2O_3 and GdF_3, respectively, in stoichiometric mixtures of KF and MgF_2 dehydrated powders. The concentration of the dopant in the melt varied in the range of 0.1−1.0 mol %. The crystals were transparent. Polished pieces of 5 × 6 × 7 mm size were used for the measurements. Previous experiments showed that doping $KMgF_3$ with Eu^{3+} ions is extremely difficult if the crystal growth is not carried out in an oxidizing atmosphere.[18] This is evidently caused by a quantitative reduction process to Eu^{2+} ions during the incorporation in the perovskite lattice, which contains practically only divalent ions of the dopant. In the present study, we used crystals grown from a melt containing 1.0 mol % Eu^{2+} ions, which is sufficiently doped to observe the weak $f^7 \rightarrow f^7$ absorption bands. Our absorption and emission spectra showed that the crystals did not contain Eu^{3+} ions.

Absorption spectra were obtained with a model 8452A diode array spectrophotometer. High-resolution emission spectra were recorded using a Spex model 1403 double monochromator equipped with a Spex model DM1B controller and a Hamamatsu R928 photomultiplier tube. Excitation wavelengths at 356.4, 350.9, and 337.5 nm were provided by a coherent model Innova-100-K3 krypton ion laser. Excitation at 354.5 nm was obtained from the third harmonic of a Quanta-Ray (Spectra-Physics) model DCR-3 Nd:YAG laser (operated at 20 Hz).

For lifetime measurements, a frequency-doubled dye laser (Lambda Physik Scanmate 2E) operating on rhodamine 101 dye and pumped by the second harmonic of a Nd:YAG laser operating at 10 Hz was used as the excitation light source. After frequency doubling, this dye laser generates light pulses of about 3 mJ total energy at a wavelength of 308 nm. The spectral bandwidth is about 0.05 cm^{-1} (fwhm) in a Gaussian envelope.

The crystal samples were fitted into a cryogenic system (Janis Research) with capabilities of automatic temperature control to measure lifetimes at different temperatures. The fluorescence photons were collected using a CaF_2 lens system and focused onto the entrance slit of a low-dispersion-power monochromator with an estimated resolution of 3 nm, and then focused onto the cathode of a photomultiplier tube (PMT) using a fiber optical assembly.

III. Results and Discussion

A. Four-Level Decay Model and the Derivation of the Fitting Equation. In this section, we will concentrate on the decay pattern of the first excited state of the $^6P_{7/2}$ energy level of the Eu^{2+} ion. After excitation into the higher $4f^65d$ manifold, Eu^{2+} experiences a rapid, nonradiative decay to the lowest excited $4f^7$ multiplet, and at low temperature fluorescence is almost entirely emitted from the $^6P_{7/2}$ state, the lowest component of the ^6P_J multiplet. When the temperature is increased, fluorescence has also been observed from the $^6P_{5/2}$ component.[7] In general, the electronically excited Eu^{2+} ion in its excited state dissipates the excess energy via internal deactivation processes, which include radiative decay, nonradiative decay, and thermal population to a higher energy level, and via intersystem crossing, which includes electron transfer and energy transfer. Given the fact that the $^6P_{5/2}$ emission is observable at 77 K,[7] the $^8S_{7/2} \rightarrow {}^6P_{3/2}$ absorption band is not observed due to the selection rule $\Delta J = 0, 1$,[1] and the lowest $4f^65d$ levels are just 100 cm^{-1} above the $4f^7$

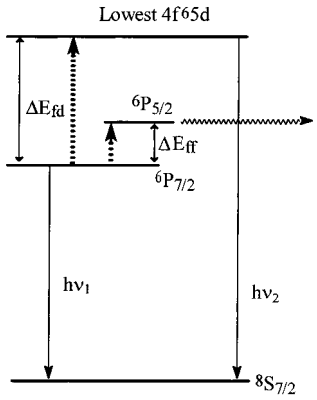

Figure 1. Four-level decay pattern of the $^6P_{7/2}$ excited state of Eu^{2+} in $KMgF_3$:Eu^{2+}: (dotted arrow) thermal population, (solid arrow) radiative transition, (wavy arrow) intersystem crossing.

(^6I) multiplets,[3] we assume that the $^6P_{5/2}$ level should be taken into account as a thermal population level upon considering the $^6P_{7/2}$ decay path. It is reasonable to consider the lowest $4f^65d$ level as a second thermally populated energy level of the $^6P_{7/2}$ state because all the higher $4f^65d$ excited states rapidly relax to the lowest $4f^65d$ energy level. On the basis of the above analysis, we propose a four-level decay pattern of the $^6P_{7/2}$ excited state, which is shown in Figure 1.

According to the three-level model, the decay time (τ) of the Eu^{2+} luminescence consisting of 4f−4f line emission and 5d−4f band emission can be described by[19,20]

$$\tau^{-1} = \frac{w_f + (g_d/g_f)w_d \exp(-\Delta E/KT)}{1 + (gd/gf)\exp(-\Delta E/KT)} \quad (1)$$

where g_d , g_f and w_d , w_f are the degeneracies and radiative probabilities of the lowest $4f^65d$ level and of the lowest excited 4f level, respectively.

According to ref 12 the decay time of the Eu^{2+} emission in $KMgF_3$ can be described by

$$1/\tau = w_f + w_d \exp(-\Delta E/KT) \quad (2)$$

This equation follows from eq 1 by using the approximations $g_d = g_f$ and $\exp(-\Delta E/KT) \ll 1$.

For the four-level system, another exponential term is needed, and eq 2 can be rewritten as

$$1/\tau = w_f + w_{ff}\exp(-\Delta E_{ff}/KT) + w_d \exp(-\Delta E_{fd}/KT) \quad (3)$$

Deactivation of the $^6P_{7/2}$ emitting states can take place via radiative decay and nonradiative decay. For Eu^{2+}, the probability of nonradiative decay between any of the excited states and the ground state is negligibly small and is neglected, due to the large energy difference (about 28000 cm^{-1}) between the $^8S_{7/2}$ state and the excited state.[24]

Thermal activation of the $^6P_{5/2}$ state and the lowest $4f^65d$ states leads to the opening of two additional energy dissipation pathways. In eq 3, the deactivation rate constant of the thermally populated $4f^65d$ states is

(18) Bacci, C.; Fioravanti, S.; Furetta, C.; Missori, M.; Ramogida, G.; Rossetti, R.; Sanipoli, C.; Scacco, A. *Radiat. Prot. Dosim.* **1993**, *47*, 277.

(19) Hewes, R. A.; Hoffman, M. V. *J. Lumin.* **1971**, *3*, 261.

(20) Sommerdijk, J. L.; Verstegen, J. M. P. J.; Bril, A. *J. Lumin.* **1975**, *10*, 411.

Table 1. Lifetime of the $^6P_{7/2}$ Emitting State of Eu^{2+} in $KMgF_3$ at Different Temperatures

Eu^{2+} (1 mol %)		$Eu^{2+}-Gd^{3+}$ (1, 0.1 mol %)		$Eu^{2+}-Ge^{3+}$ (1, 0.1 mol %)		$Eu^{2+}-Cr^{3+}$ (1, 0.5 mol %)	
T (K)	τ (ms)	T (K)	τ (ms)	T (K)	τ (ms)	T (K)	τ (ms)
87.0	3.49	87.9	3.31	88.8	3.37	88.7	3.53
100.1	3.50	106.6	3.29	102.0	3.29	101.6	3.47
155.0	3.37	150.7	3.19	150.8	3.02	150.4	3.24
203.9	2.99	199.6	2.98	204.7	2.79	199.3	3.05
253.0	2.75	249.0	2.83	250.8	2.70	248.0	2.82
300.2	2.63	300.1	2.63	295.8	2.52	298.5	2.57
367.1	2.22	346.9	2.40	348.5	2.27	350.4	2.31
461.0	1.52	440.1	1.68	438.9	1.61	450.2	1.81

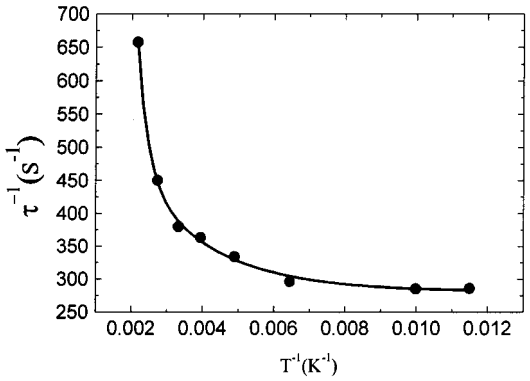

Figure 2. Fitting curve of $KMgF_3:Eu^{2+}$ (1 mol %). The solid circle represents the experimental data. The drawn line is a fit based on eq 3 with $w_f = 281 s^{-1}$, $w_{ff} = 499\ s^{-1}$, $w_d = 2.8 \times 10^5\ s^{-1}$, $\Delta E_{ff} = 324\ cm^{-1}$, and $\Delta E_{fd} = 2282\ cm^{-1}$.

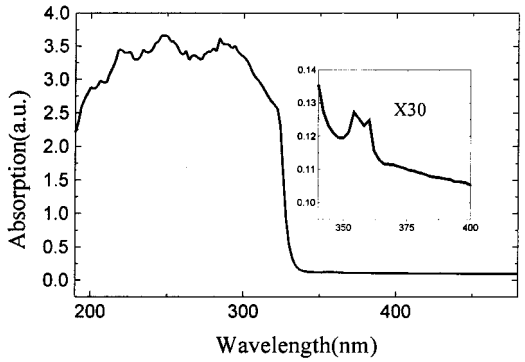

Figure 3. Absorption spectrum of $KMgF_3:Eu^{2+}$ at room temperature. The inset is the $^6P_{7/2}$ and $^6P_{5/2}$ absorption region magnified 30 times.

designated w_d and equals the radiative probabilities of the lowest $4f^65d$ level. ΔE_{fd} is the energy gap between the lowest $4f^65d$ states and the $^6P_{7/2}$ emitting states. The deactivation rate constant (w_{ff}) is associated with the low-lying $^6P_{5/2}$ state, which may be thermally populated as a consequence of the small magnitude of ΔE_{ff}, and its physical implication will be discussed later.

w_f represents the rate constant for direct radiative decay of the $^6P_{7/2}$ state. On the basis of the literature,[3] it should contain contributions from the transition probability of the vibrational states (Stokes and anti-Stokes), and thus, w_f in eq 3 consists of two terms:

$$w_f = A_{vib} + A_{zp} \tag{4}$$

In eq 4 A_{vib} gives the contribution of the vibronic (vib) transitions to the total radiative transition probability (w_f) of the excited state $^6P_{7/2}$. A_{zp} represents the radiative transition probability of the zero-phonon (zp) line (359.3 nm).

B. Fitting Results and Spectral Data. Table 1 presents the lifetime data in the temperature regime 80−450 K for different samples. Fitting the data of $KMgF_3:Eu^{2+}$(1 mol %) to eq 3, we obtained the related parameters as $w_f = 281\ s^{-1}$, $w_{ff} = 499\ s^{-1}$, $w_d = 2.8 \times 10^5\ s^{-1}$, $\Delta E_{ff} = 324\ cm^{-1}$, and $\Delta E_{fd} = 2282\ cm^{-1}$. Figure 2 shows that the experimental decay data can be fitted quite well to eq 3. w_d is in good agreement with the reported data 6×10^5 and $8 \times 10^5\ s^{-1}$ (calculated from the lifetime of 1.2 μs) for Eu^{2+} 5d−4f transitions.[6,20]

The absorption spectrum of $KMgF_3:Eu^{2+}$ (1 mol %) at room temperature is shown in Figure 3. The absorption due to the $^8S_{7/2} \rightarrow {}^6P_{5/2}$ and $^8S_{7/2} \rightarrow {}^6P_{7/2}$ transitions at 354 and 360 nm, respectively, are observed, as reported by Tsuboi et al.[1] From the onset of the $4f^65d$, $^6P_{7/2}$, and $^6P_{5/2}$ absorption bands, ΔE_{ff} and ΔE_{fd} can be estimated for $KMgF_3:Eu^{2+}$. The values are 324 and 2233 cm^{-1}, respectively. Again, these data are in good agreement with the fitting results.

As can be seen from the absorption results, there are some differences between our data and the reported values for ΔE_{fd}, i.e., 1250 cm^{-1} by Sardar et al.,[5] 120 cm^{-1} by Altshuler et al.,[12] and 3350 cm^{-1} by Ellens et al.[3] What is the reason for this difference? Our detailed study shows that the type of model used in the calculation is one factor. Another important factor that affects the $4f^65d$ level position is the oxygen content in the crystals. Since fluoride possesses the pyrohydrolysis property (interaction with water vapor in the crystal growth process), one can suppose that oxygen-containing impurities in $KMgF_3$ play a very important role.[2] As reported in the literature,[4,11,21] the position of the $4f^65d$ state depends on the covalency and crystal field strength at the Eu^{2+} site. Introducing oxygen into the crystal will increase the covalency and crystal field strength at the Eu^{2+} site. As a result the center of gravity of the $4f^65d$ states is shifted to lower energy. That traces of oxygen impurities exist in our crystals is clearly shown in the absorption spectra (Figure 3) at 204 and 224 nm as reported.[22,23] Thus, it is reasonable that the value of ΔE_{fd} from our results is smaller than that reported by Ellens et al.[3]

Figure 4 illustrates the contributions from each term in eq 3 to the total transition probability. As can be seen, at room temperature, the dominant contribution for the total transition probability is from the $^6P_{7/2}$ emission, 27% of the energy is lost via the $^6P_{5/2}$ decay path, and

(21) Blasse, G. *Phys. Status Solidi B* **1973**, *55*, K131.
(22) Gektin, A. V.; Komar, V. K.; Shiran, N. V.; Shlykhturov, V. V.; Nesterenko, N. P.; Krasovitskaya, I. M.; Kornienko, V. V. *IEEE Trans. Nucl. Sci.* **1995**, *42*, 311.
(23) Gektin, A. V.; Krasovitskaya, I. M.; Shiran, N. V. *Radiat. Meas.* **1998**, *29*, 337.
(24) Meijerink, A. *J. Lumin.* **1993**, *55*, 125.

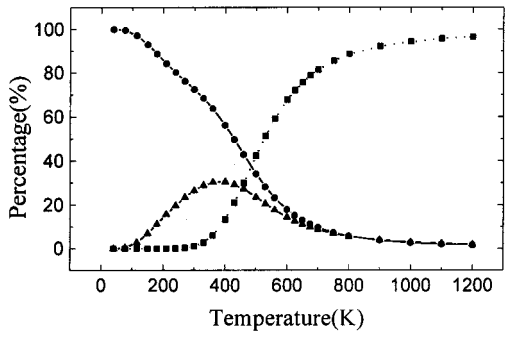

Figure 4. Contributions to the total transition probability ($1/\tau$) from each term in eq 3. The solid circle represents the percentage of w_f, the solid triangle corresponds to the percentage of the $w_{ff}\exp(-\Delta E_{ff}/KT)$ term, and the solid square is the percentage of the term $w_d\exp(-\Delta E_{fd}/KT)$. The lines drawn through the data points are a guide to the eye.

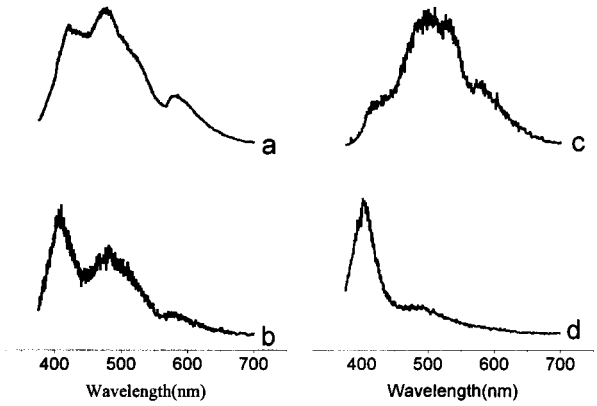

Figure 5. Emission spectra of $KMgF_3:Eu^{2+}$ excited with a laser at (a) 356.4 nm at room temperature, (b) 350.9 nm at room temperature, (c) 350.9 nm at 77 K and (d) 337.5 nm at room temperature.

the $4f^65d$ emission can be neglected in this case. With an increase of temperature, the $4f^65d$ emission gradually dominates the spectra, and at 650 K a 77% contribution is from this level and the line emission intensity becomes negligible. This result agrees well with the reported one.[5]

It is important to note how the $^6P_{5/2}$ level loses its energy after it is thermally populated. Releasing energy through nonradiative decay to the $^8S_{7/2}$ ground state is impossible because of the large energy gap between the $^6P_{7/2}$ and $^8S_{7/2}$ states. Another possible path is through direct emission, but this possibility is excluded by the fact that the $^6P_{5/2}$ emission is not available above 77 K in our crystal. The third possibility is that the $^6P_{5/2}$ state thermally populates the $4f^65d$ level. If this is the case, the two exponential decays in eq 3 become unnecessary. On the basis of the above analysis, we conclude that the $^6P_{5/2}$ state is a special energy dissipation pathway. The preexponential factor w_{ff} represents the dissipation coefficient. At about 400 K (Figure 4), the energy loss via the $^6P_{5/2}$ channel reaches its maximum. Taking into account the thermoluminescence at 390 K described in the literature,[22,23] we assume that the lost energy is most possibly related to the energy transfer to the F_n color and oxygen centers in the crystal by intersystem crossing. Our emission spectra (see Figure 5) excited with different wavelengths of the UV-laser beam demonstrate the existence of O^{2-} and F_n centers. As described in the literature,[23,26] a complex emission spectrum consisting of overlapping bands in the range of 370−700 nm is connected with intrinsic point defects and oxygen impurity contents.

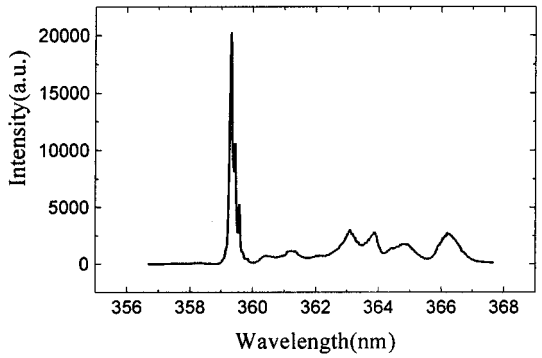

Figure 6. Emission spectrum of $KMgF_3:Eu^{2+}$ excited with a 350.9 nm laser at 77 K.

An important fact to support the above argument is the intensity ratio of line (360 nm) to band (370−700 nm) emission. At room temperature, the energy loss via the $^6P_{5/2}$ state almost reaches its maximum. The $KMgF_3:Eu-X$ (X = Gd, Ce, Cr) codoped system can considerably change the value of w_{ff} (vide infra, Table 4). If energy transfer from the $^6P_{5/2}$ state to the F_n and oxygen centers exists, then introducing Gd^{3+} and Ce^{3+} will lower the intensity of the F_n and oxygen centers, whereas introducing Cr^{3+} will result in an increase of the intensity of the F_n and oxygen centers. Calculating the ratios of the integral intensities of the line to band emission from emission spectra at room temperature, we found values of 0.20, 0.19, and 0.13 for X = Gd, Ce, and Cr, respectively. The ratio for $KMgF_3:Eu^{2+}$ is 0.15. The order of these ratios is in good agreement with the values expected. We also note that, with a decrease in temperature (Figure 5b,c), the emission intensity of the deep trap (500 nm) and O^{2-} (530 nm) centers increases, whereas the intensity of the emission related to point defects (407, 470, and 580 nm) decreases. At 77 K, no contribution from $^6P_{5/2}$ can be obtained. As a result, the emission intensity of some point defects decreases or disappears (407 nm).

When the temperature is held at 77 K, there are almost no contributions from $^6P_{5/2}$ and $4f^65d$ thermally populated decay. An energy of 99.7% emits radiatively via the $^6P_{7/2}$ excited state. Then, the two exponential terms in eq 3 can be neglected, and eq 3 becomes

$$1/\tau = w_f = A_{vib} + A_{zp} \tag{5}$$

In eq 5, A_{vib} gives the contribution of the vibronic transitions to the total radiative transition probability (w_f) of the $^6P_{7/2}$ excited state. The ratio of the total vibronic intensity to the total zero-phonon line intensity is given by

$$R = I_{vib}/I_{zp} = A_{vib}/A_{zp} \tag{6}$$

From the R value and the decay time, the vibronic and zero-phonon transition probabilities (A_{vib} and A_{zp}) can be obtained by eqs 5 and 6.[3,24,25] Using the R value from

(25) Sytsma, J.; Imbusch, G. F.; Blasse, G. *J. Chem. Phys.* **1989**, *91*, 1456.

Table 2. w_f Values Obtained from the Fit and Emission Spectra

sample	w_f (s^{-1}) fit	w_f (s^{-1}) calcd	sample	w_f (s^{-1}) fit	w_f (s^{-1}) calcd
Eu^{2+} (1 mol %)	281 ± **2**	287	Eu^{2+}−Ce^{3+} (1, 0.1 mol %)	304 ± 3	298
Eu^{2+}−Gd^{3+} (1, 0.1 mol %)	300 ± **1**	302	Eu^{2+}−Cr^{3+} (1, 0.5 mol %)	283 ± 1	282

Table 3. Calculated ΔE_{ff} and ΔE_{fd} from Absorption Spectra

sample	ΔE_{ff} (cm^{-1})	ΔE_{fd} (cm^{-1})
Eu^{2+}−Gd^{3+} (1, 0.1 mol %)	324	2139
Eu^{2+}−Ce^{3+} (1, 0.1 mol %)	324	1850
Eu^{2+}−Cr^{3+} (1, 0.5 mol %)	324	1850

Table 4. Fit Parameters from Eq 3 for Different Crystals

sample	w_f (s^{-1})	w_{ff} (s^{-1})	$10^5 w_{fd}$ (s^{-1})
Eu^{2+} (1 mol %)	281	499	2.8
Eu^{2+}−Gd^{3+} (1, 0.1 mol %)	300	358	2.1
Eu^{2+}−Ce^{3+} (1, 0.1 mol %)	304	422	0.8
Eu^{2+}−Cr^{3+} (1, 0.5 mol %)	283	503	0.4

the emission spectrum (Figure 6) and the lifetime at 77 K, i.e., $\tau = 3.49$ ms and $R = 2.2$ (integral intensity ratio), we obtained $A_{zp} = 89\ s^{-1}$ and $A_{vib} = 198\ s^{-1}$. Thus, $w_f = A_{vib} + A_{zp} = 287\ s^{-1}$. Similarly, the values of the other crystals can be calculated and are shown in Table 2. As can be seen, all values agree well with those obtained from the fitting result.

Summarizing, the temperature dependence of the lifetime of the Eu^{2+} $^6P_{7/2}$ luminescence in $KMgF_3$:Eu^{2+} and $KMgF_3$:Eu^{2+}−X (X = Gd, Ce, Cr) has been measured in the temperature range of 80−460 K. All of the data can be well fit to a biexponential decay equation. A four-level decay model responsible for the fit equation was proposed. The fit results for ΔE_{ff} and ΔE_{fd} for $KMgF_3$:Eu^{2+} are in good agreement with the data obtained spectroscopically. The reason for the ΔE_{fd} differences from different laboratories is suggested to be differences in the calculation method and oxygen content in the sample. The radiative transition probability of the $4f^65d$ excited state agrees with the reported value. Vibronic and zero-phonon transition probabilities of the $^6P_{7/2} \rightarrow {}^8S_{7/2}$ transition of Eu^{2+} in $KMgF_3$ were calculated. An important energy dissipation pathway from the $^6P_{5/2}$ excited state was found, and it is most likely related to the intrinsic point defects and oxygen centers in the crystal.

C. Study of Energy Transfer Using the Four-Level Model in $KMgF_3$:Eu−X (X = Gd, Ce, Cr). From absorption spectra, ΔE_{ff} and ΔE_{fd} can be estimated for three other crystals and are presented in Table 3.

Introducing these data into eq 3 and then fitting the data in Table 1, we obtained all of the parameters, which are shown in Table 4.

Table 4 shows that doping with other impurity ions considerably affects all the transition probability terms in eq 3. Comparing Gd−Eu and Ce−Eu codoped $KMgF_3$ with $KMgF_3$:Eu^{2+}, we found that w_f is increased whereas w_{ff} and w_d are decreased. These results clearly indicate that energy transfer from Gd^{3+} and Ce^{3+} to the f−f level of the Eu^{2+} ion takes place in the studied systems. On the other hand, doping the crystal with Cr^{3+}−Eu^{2+} results in almost the same w_f and w_{ff} as those for $KMgF_3$:Eu^{2+}, which indicates no influence of Cr^{3+} doping on the f−f luminescence (total luminescence of the zero-phonon and vibronic transitions) of the Eu^{2+} ion. However, doping the crystal with Cr^{3+}−Eu^{2+} reduced the $4f^65d$ transition probability by a factor of 7, which implies that energy transfer happens from the $^6P_{7/2}$ level of Eu^{2+} to the 3d level of Cr^{3+}. It is interesting to note that the $4f^65d$ transition probability (w_d) is gradually decreased in the order Gd, Ce, and Cr, which results from d−d interaction between Eu^{2+} and these ions and has been discussed in more detail elsewhere.[27]

To verify the energy transfer described above, we conducted a series of emission measurements excited at different wavelengths and calculated their relative integral intensity, which is presented in Table 5.

Table 5 shows that doping $KMgF_3$ with Eu^{2+}−Gd^{3+} and Eu^{2+}−Ce^{3+} significantly increases the total intensity (I_t) of the zero-phonon and vibronic transitions of the Eu^{2+} ion. But doping with Cr^{3+} has no effect on the I_t of $KMgF_3$:Eu^{2+}. Thus, the spectral data support the results from the fit. Table 5 also demonstrates that the percentage of zero-phonon transition emission of Eu^{2+} is decreased upon doping $KMgF_3$ with Eu^{2+}−Gd^{3+}, Eu^{2+}−Ce^{3+}, and Eu^{2+}−Cr^{3+}, which implies that the vibronic transition emission (I_{vib}) is increased with the doping of other mentioned ions. These results suggest that energy transfer from Gd^{3+} and Ce^{3+} to Eu^{2+} occurs in $KMgF_3$:Eu−Gd and $KMgF_3$:Eu−Ce, but the energy is transferred to the vibronic transition. As described previously, the vibronic transition probability (A_{vib}) and zero-phonon transition probability (A_{zp}) can be calculated from eqs 5 and 6 at 77 K. In fact, at any temperature, the fit parameter w_f represents the total contribution from A_{vib} and A_{zp}, but the ratio of A_{vib} to A_{zp} varies with temperature. Therefore, the values of A_{vib} and A_{zp} at any temperature can be calculated on the basis of the emission spectra ($R = I_{vib}/I_{zp}$) and fit parameter ($w_f = A_{vib} + A_{zp}$). The calculated results at 77 and 300 K are presented in Table 6. It clearly shows that the energy from Gd^{3+} or Ce^{3+} is transferred to the vibronic transition of Eu^{2+}. For the $KMgF_3$:Eu−Cr system, although the total transition probability w_f is the same as that of $KMgF_3$:Eu^{2+}, i.e., no energy transfer from Cr^{3+} to the f−f level of Eu^{2+}, the zero-phonon transition probability is considerably decreased and the vibronic transition probability is increased.

Another interesting result can be drawn from the data of Table 5. When Eu^{2+} is excited at 350.9 nm into its $^6P_{5/2}$ manifold at 77 K, the total intensity (I_t) of $KMgF_3$:Eu−Gd is two times greater than that of $KMgF_3$:Eu. At 77 K, the thermal population of $^6P_{5/2}$ and $4f^65d$ can be neglected (Figure 4), and the only decay path of the $^6P_{5/2}$ excited state is the relaxation to the $^6P_{7/2}$ excited state or the direct energy loss through the $^6P_{5/2}$ pathway. Thus, $KMgF_3$:Eu^{2+} will lose much more energy than $KMgF_3$:Eu^{2+}−Cd^{3+} via the $^6P_{5/2}$ pathway

(26) Shkadarevich, A. P.; Dubinskii, M. A.; Nikanovich, M. V.; Silkin, N. I.; Umreiko, D. S.; Yagudin, Sh. I.; Yarmolkevich, A. R. *Opt. Commun.* **1986**, *57*, 400.

(27) Su, H. Q.; Jia, Z. H.; Shi, C. S.; Xin, J.; Reid, S. A. *Chem. Phys. Lett.*, in press.

Table 5. Relative Emission Intensity of Zero-Phonon and Vibronic Transitions of Eu^{2+} in Different Crystals

laser excitation wavelength (nm)	Eu^{2+} (1 mol %)		Eu^{2+}–Gd^{3+} (1, 0.1 mol %)		Eu^{2+}–Ce^{3+} (1, 0.1 mol %)		Eu^{2+}–Cr^{3+} (1, 0.5 mol %)	
	I_t[a]	I_{zp}[b] (%)	I_t	I_{zp} (%)	I_t	I_{zp} (%)	I_t	I_{zp} (%)
350.9	720	28			1800	24		
350.9[c]	5800	31	12000	23				
337.5	6.4×10^6	27			2.1×10^8	27		
354.5	99	25			102	24	100	23
356.4	590	25			4700	25		

[a] Total intensity of the zero-phonon (360 nm) and vibronic transitions. [b] Intensity of the zero-phonon transition. $I_t = I_{vib} + I_{zp}$. I_{zp} (%) $= I_{zp}/I_t \times 100$. [c] Emission at 77 K.

Table 6. Calculated Vibronic and Zero-Phonon Transition Probabilities from Emission Spectra and the Fit Equation

sample	300 K		77 K	
	A_{vib}	A_{zp}	A_{vib}	A_{zp}
Eu^{2+} (1 mol %)	203	78	194	87
Eu^{2+}–Gd^{3+} (1, 0.1 mol %)	224	76	232	67
Eu^{2+}–Ce^{3+} (1, 0.1 mol %)	230	75	216	89
Eu^{2+}–Cr^{3+} (1, 0.5 mol %)	218	64		

because of the larger w_{ff} value of the former, which results in weaker emission of $KMgF_3$:Eu^{2+}.This result strongly supports the fact that the $^6P_{5/2}$ channel exists in the $KMgF_3$:Eu−X system.

To summarize, we have described the application of a four-level model in studying the energy transfer between Eu^{2+} and Ce^{3+}, Gd^{3+} in the $KMgF_3$ host. The energy-transfer mechanism and the energy dissipation path are well explained by this model. Ce^{3+} and Gd^{3+} are good sensitizers for the vibronic transition of Eu^{2+} in $KMgF_3$.

IV. Conclusion

The temperature dependence of the lifetime of the Eu^{2+} $^6P_{7/2}$ emission in $KMgF_3$:Eu−X (X = Gd, Ce, Cr) and $KMgF_3$:Eu in the range of 80−460 K can be well fit to a biexponential decay equation. A four-level decay model responsible for the fit equation was proposed. On the basis of this model, the energy difference between $4f^65d$ and $^6P_{7/2}$, $^6P_{5/2}$ and $^6P_{7/2}$ can be obtained from the fit. The reason for the different values of the energy difference between $4f^65d$ and $^6P_{7/2}$ with different authors is attributed to differences in the calculation method and oxygen impurity content in the crystal. The $4f^65d$ transition probability and vibronic and zero-phonon transition probabilities of the $^6P_{7/2} \rightarrow {}^8S_{7/2}$ transition of Eu^{2+} in $KMgF_3$ above 77 K can be calculated from fit parameters and emission spectra. An important energy dissipation pathway from the $^6P_{5/2}$ excited state was found, and it is most likely related to the intrinsic point defects and oxygen centers in the crystal.

The energy-transfer mechanism in the codoped $KMgF_3$ system can be studied by the measurement of the temperature dependence of the lifetime on the basis of the four-level decay model. Doping $KMgF_3$ with Eu^{2+}–Gd^{3+} and Eu^{2+}–Ce^{3+} increases the vibronic transition probability of the $^6P_{7/2} \rightarrow {}^8S_{7/2}$ transition of Eu^{2+}. Introducing Cr^{3+}–Eu^{2+} into $KMgF_3$ results in a decrease of the zero-phonon transition probability of the Eu^{2+} ion.

Acknowledgment. We thank Xianming Zhang and Chunyu Zang for their assistance in the experiment setup and sample preparation for the crystal growth. We also thank Dr. James R. Kincaid of the Chemistry Department of Marquette University for providing the setup used to obtain high-resolution emission spectra. This work was supported by the national key project of China for fundamental research.

CM0101881